SOI: 1.1/TAS DOI: 10.15863/TAS

International Scientific Journal
Theoretical & Applied Science

p-ISSN: 2308-4944 (print) **e-ISSN:** 2409-0085 (online)

Year: 2017 **Issue:** 09 **Volume:** 53

Published: 9.09.2017 **http://T-Science.org**

Denis Chemezov
Master of Engineering and Technology,
Corresponding Member of International Academy of Theoretical and Applied Sciences, Lecturer of Vladimir Industrial College, Russian Federation
chemezov-da@yandex.ru

SECTION 6. Metallurgy and energy.

THE MATHEMATICAL MODELS OF SHRINKAGE FORMATION IN METALLIC ALLOYS

***Abstract**: A mathematical description of shrinkage formation in different metallic alloys from temperature of melt, time and cooling rate is given. The values of shrinkage were obtained in liquid and in solid phases of sixteen metallic alloys at cooling time up to 70 minutes.*

***Key words**: shrinkage, a regression equation, temperature, time, cooling rate, alloy.*
***Language**: English*
***Citation**:* Chemezov D (2017) THE MATHEMATICAL MODELS OF SHRINKAGE FORMATION IN METALLIC ALLOYS. ISJ Theoretical & Applied Science, 09 (53): 23-42.
Soi: http://s-o-i.org/1.1/TAS-09-53-5 ***Doi***: crossref https://dx.doi.org/10.15863/TAS.2017.09.53.5

Introduction

Many scientific works are dedicated by the research of the formation of shrinkage defects in metallic castings when cooling [1; 2; 3; 4; 5; 6; 7; 8]. The experiments in the industrial conditions and the computer modeling allow to obtain the reliable results of the casting process and perform the analysis of the formation in material of the shrinkage defects. The change of linear or volumetric shrinkage of the casting from temperature of alloy and cooling time can be represented by the regression equations.

Materials and methods

The computer calculation of cooling of metallic alloys and the analysis of the results were carried out in the programs LVMFlow and STATISTICA.

The research of the cooling process was performed for following alloys: alloy steel 34CrMo4; quality carbon steel 1.0503; corrosion-resistant steel X3CrNiMo18-12; chromium steel SIS.2302; grey cast iron EN-GJL-150; malleable cast iron EN-JGS-600-3; wear-resistant cast iron EN-GJMW-210 (ductile cast iron); tinless bronze CuAl10Fe2-C; tin bronze CuSn5Zn5Pb5-C; brass CuZn40; aluminium foundry alloy SG 70A (silumin); zinc alloy ZA-8; nickel-cobalt alloy num.1; magnesium alloy MAG2; heat-resistant nickel alloy NiCr20TiAl; precise soft magnetic alloy 49K2FA. The chemical composition of metallic alloys is presented in table 1.

Table 1

The chemical composition of alloys.

Name of alloy	Alloying elements, %																			
	Fe	C	Si	Mn	Cr	P	S	Cu	Ni	Al	Mo	Sn	Zn	Pb	Mg	Ti	Cd	Co	Ce	V
34CrMo4	96.58	0.35	0.3	0.65	0.95	0.04	0.04	0.3	0.5	0.04	0.25	-	-	-	-	-	-	-	-	-
1.0503	97.775	0.46	0.27	0.65	0.25	0.035	0.04	0.25	0.25	0.02	-	-	-	-	-	-	-	-	-	-
X3CrNiMo18-12	72.37	0.03	0.8	0.8	16	-	-	-	10	-	-	-	-	-	-	-	-	-	-	-
SIS.2302	85.71	0.14	0.19	0.68	12	0.02	0.01	0.03	1.2	-	0.02	-	-	-	-	-	-	-	-	-
EN-GJL-150	93.22	3.55	2.35	0.65	-	0.15	0.08	-	-	-	-	-	-	-	-	-	-	-	-	-
EN-JGS-600-3	92.96	3.3	2.4	0.4	0.15	0.08	0.01	0.3	0.4	-	-	-	-	-	-	-	-	-	-	-
EN-GJMW-210	63.2	2	1	0.7	30	0.1	0.1	-	2.9	-	-	-	-	-	-	-	-	-	-	-
CuAl10Fe2-C	3	-	-	-	-	-	-	87	1	9	-	-	-	-	-	-	-	-	-	-
CuSn5Zn5Pb5-C	-	-	-	-	-	-	-	85	-	-	-	5	5	5	-	-	-	-	-	-
CuZn40	-	-	-	-	-	-	-	60	-	-	-	-	40	-	-	-	-	-	-	-
SG 70A	0.28	-	7.5	0.3	-	-	-	-	-	91.68	-	-	0.03	-	0.2	0.01	-	-	-	-
ZA-8	0.07	-	-	-	-	-	-	1	-	8.4	-	-	90.49	0.01	0.02	-	0.01	-	-	-
num.1	-	-	-	-	-	-	-	-	80	-	-	-	-	-	-	-	-	20	-	-
MAG2	-	-	-	0.22	-	-	-	-	-	8.1	-	-	0.7	-	90.98	-	-	-	-	-
NiCr20TiAl	1	0.06	0.06	0.4	20.5	-	-	-	74.32	0.95	-	-	-	-	-	2.7	-	-	0.01	-
49K2FA	48.75	0.03	0.15	0.3	-	0.01	0.01	-	0.3	-	-	-	-	-	-	-	-	49	-	1.85

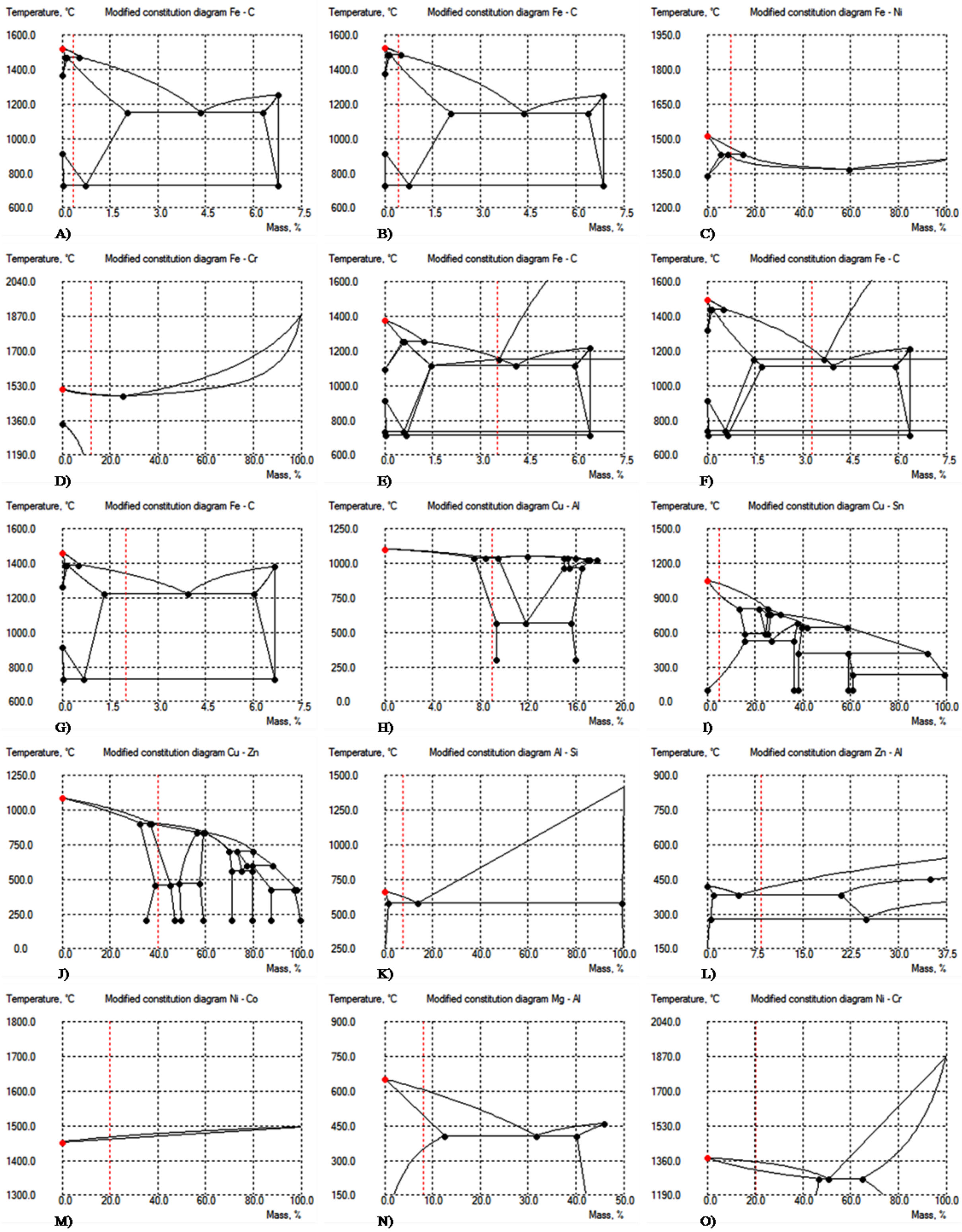

Figure 1 – The modified constitution diagrams of alloys: A – alloy steel 34CrMo4; B – quality carbon steel 1.0503; C – corrosion-resistant steel X3CrNiMo18-12; D – chromium steel SIS.2302; E – grey cast iron EN-GJL-150; F – malleable cast iron EN-JGS-600-3; G – ductile cast iron EN-GJMW-210; H – tinless bronze CuAl10Fe2-C; I – tin bronze CuSn5Zn5Pb5-C; J – brass CuZn40; K – aluminium foundry alloy SG 70A; L – zinc alloy ZA-8; M – nickel-cobalt alloy num.1; N – magnesium alloy MAG2; O – heat-resistant nickel alloy NiCr20TiAl.

Initial temperatures of melts (red dot) and the percentage of the second main element of alloy (red dotted line) are presented on the modified constitution diagrams (Fig. 1).

The simulation was implemented by the non-equilibrium calculation model which takes into account the formation of the different solid phases during solidification of alloy [9]. When cooling of corrosion-resistant steel X3CrNiMo18-12, chromium steel SIS.2302, tin bronze CuSn5Zn5Pb5-C, brass CuZn40 and nickel-cobalt alloy num.1 one solid phase is formed. When cooling of alloy steel 34CrMo4, carbon steel 1.0503, ductile cast iron EN-GJMW-210, tinless bronze CuAl10Fe2-C, aluminium foundry alloy SG 70A, zinc alloy ZA-8, magnesium alloy MAG2 and nickel alloy NiCr20TiAl two solid phases are formed. When cooling of grey cast iron EN-GJL-150 and malleable cast iron EN-JGS-600-3 three solid phases are formed. The cylindrical castings with a diameter of 20 mm were exposed by cooling.

Preset cooling time of each alloy was the criterion of auto stop. Cooling time was taken of 70 min (4200 s). The calculation time step of the cooling process of the castings was adopted of 100 s.

The value of shrinkage was calculated with accurate to fourth decimal places.

Results and discussion

Maximum cooling rate of melts is observed in the time range of 1 – 5 min. Hereinafter cooling rate of alloys is constantly decreased.

The ranges of temperature change of alloys when cooling in the course of 70 minutes are presented in table 2.

Table 2

The ranges of temperature change of alloys when cooling.

Name of alloy	The range of temperature change when cooling of alloy (70 min)
Alloy steel 34CrMo4	1590 – 296.08 °C
Carbon steel 1.0503	1580 – 297.47 °C
Corrosion-resistant steel X3CrNiMo18-12	1550 – 277.92 °C
Chromium steel SIS.2302	1580 – 289.97 °C
Grey cast iron EN-GJL-150	1250 – 201.86 °C
Malleable cast iron EN-JGS-600-3	1300 – 203.95 °C
Ductile cast iron EN-GJMW-210	1440 – 227.33 °C
Tinless bronze CuAl10Fe2-C	1130 – 101.5 °C
Tin bronze CuSn5Zn5Pb5-C	1110 – 93.78 °C
Brass CuZn40	990 – 106.59 °C
Aluminium foundry alloy SG 70A	720 – 53.06 °C
Zinc alloy ZA-8	500 – 50.64 °C
Nickel-cobalt alloy num.1	1560 – 289.24 °C
Magnesium alloy MAG2	700 – 32.18 °C
Nickel alloy NiCr20TiAl	1440 – 208.18 °C
Soft magnetic alloy 49K2FA	1550 – 145.2 °C

The three-dimensional plots of the surfaces were constructed. The surfaces were fitted (the quadratic smoothing method) to the corresponding variables in the XYZ coordinates. The description of these plots is carried out according to the obtained polynomial regression equations.

The matrix plots give an idea about the dependence between variables of some set as a matrix of conventional two-dimensional plots. These plots are described by the linear regression equations.

The graphic images of changes of the shrinkage value of alloys when cooling are presented in Figs. 2 – 17. According to the regression equations (1 – 32), shown below of the plots, the dependence of alloys shrinkage from temperature, time and cooling rate was defined.

Let's do an analysis of the results of the mathematical modelling. Cooling rate of alloys CuAl10Fe2-C, SG 70A and ZA-8 on the certain time ranges is equal to zero or maybe an increase of materials temperature. This change is expressed by multiplication of the coefficient *k* by cooling rate *v* of alloys (provided $0 < k < 1$). Since cooling time *t* for all alloys was the same then the coefficients don't change significantly with allowance for the change of temperature.

Linear shrinkage of soft magnetic alloy 49K2FA was amount to 13.1411 % from the estimated dimensions of the casting. This is in 1.2 times more of shrinkage of carbon steel 1.0503, in 1.83 times more of shrinkage of ductile cast iron EN-GJMW-210 and in 1.08 times more of shrinkage of aluminium foundry alloy SG 70A.

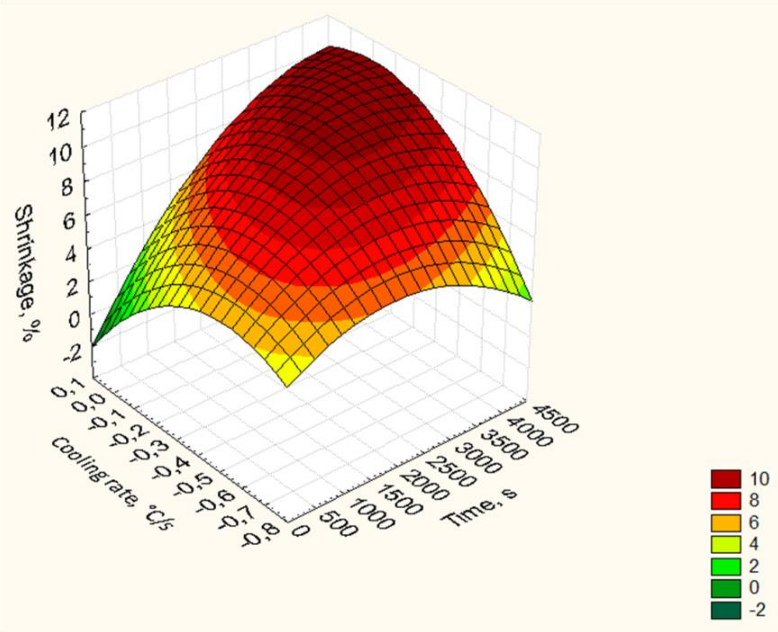

Regression equation (3D surface plot)

$$\varepsilon = 0.0049 + 0.0049t - 18.9839v - 5.7111 \cdot 10^{-7}t^2 + 0.0035tv - 17.419v^2 \quad (1)$$

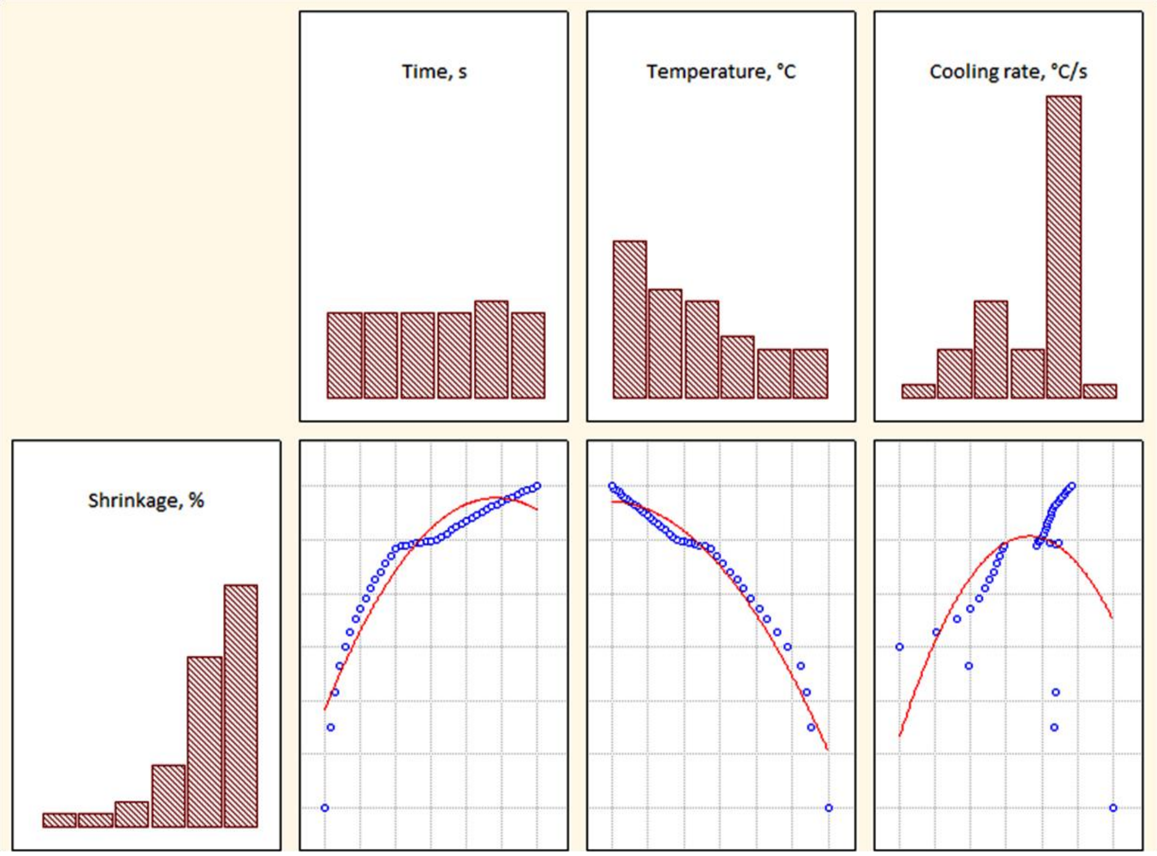

Regression equations (Matrix plot)

$$\begin{cases} \varepsilon = 5.36442019 + 0.00167739787t \\ \varepsilon = 13.7507805 - 0.00625124791T \\ \varepsilon = 10.3652473 + 5.38178652v \end{cases} \quad (2)$$

Figure 2 – The dependencies of shrinkage of alloy steel 34CrMo4 from temperature, time and cooling rate. *t* – time, s; *v* – cooling rate, °C/s; *T* – temperature, °C.

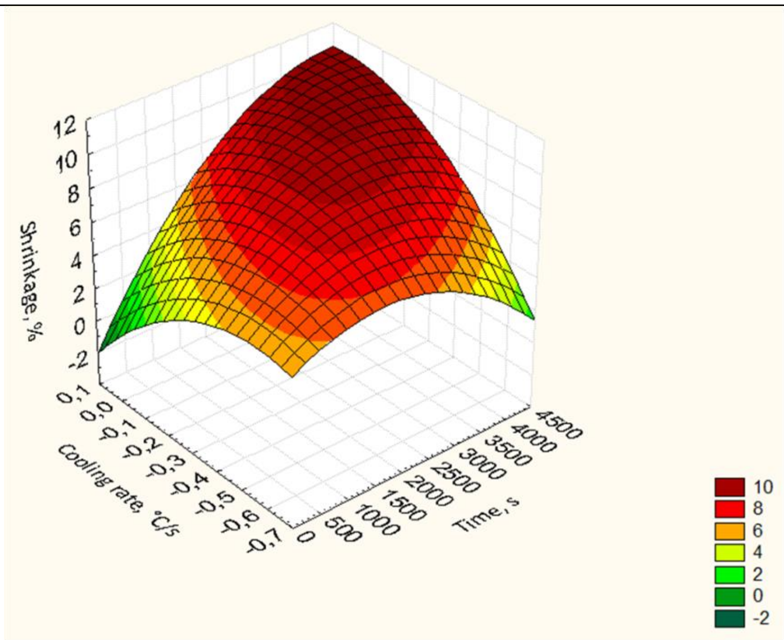

Regression equation (3D surface plot)

$$\varepsilon = 0.0085 + 0.0051t - 18.5694v - 6.1648 \cdot 10^{-7}t^2 + 0.0045tv - 16.3751v^2 \quad (3)$$

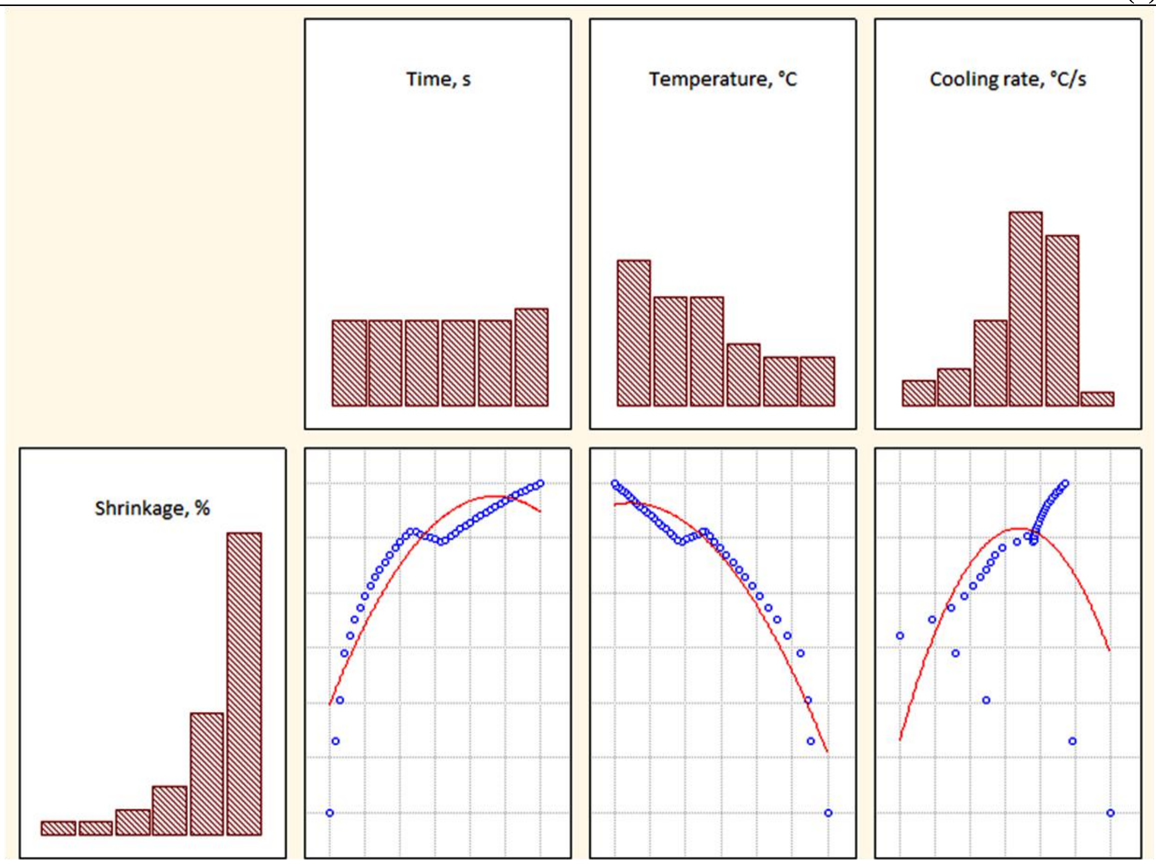

Regression equations (Matrix plot)

$$\begin{cases} \varepsilon = 5.39259266 + 0.0015041594t \\ \varepsilon = 13.0394343 - 0.00571105106T \\ \varepsilon = 9.85077189 + 4.72152743v \end{cases} \quad (4)$$

Figure 3 – The dependencies of shrinkage of carbon steel 1.0503 from temperature, time and cooling rate. *t* – time, s; *v* – cooling rate, °C/s; *T* – temperature, °C.

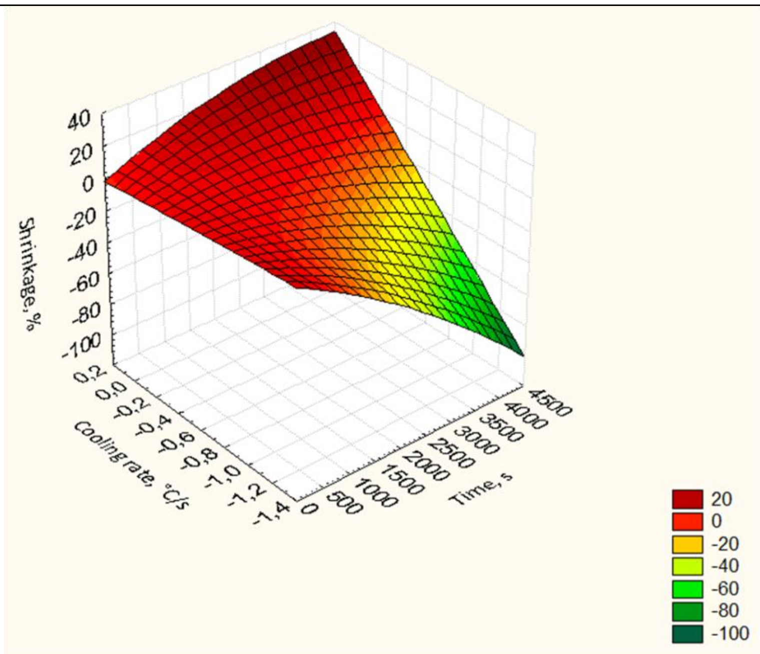

Regression equation (3D surface plot)

$$\varepsilon = 0.2429 + 0.0115t - 9.9151v - 1.7253 \cdot 10^{-6}t^2 + 0.0205tv - 1.1471v^2 \quad (5)$$

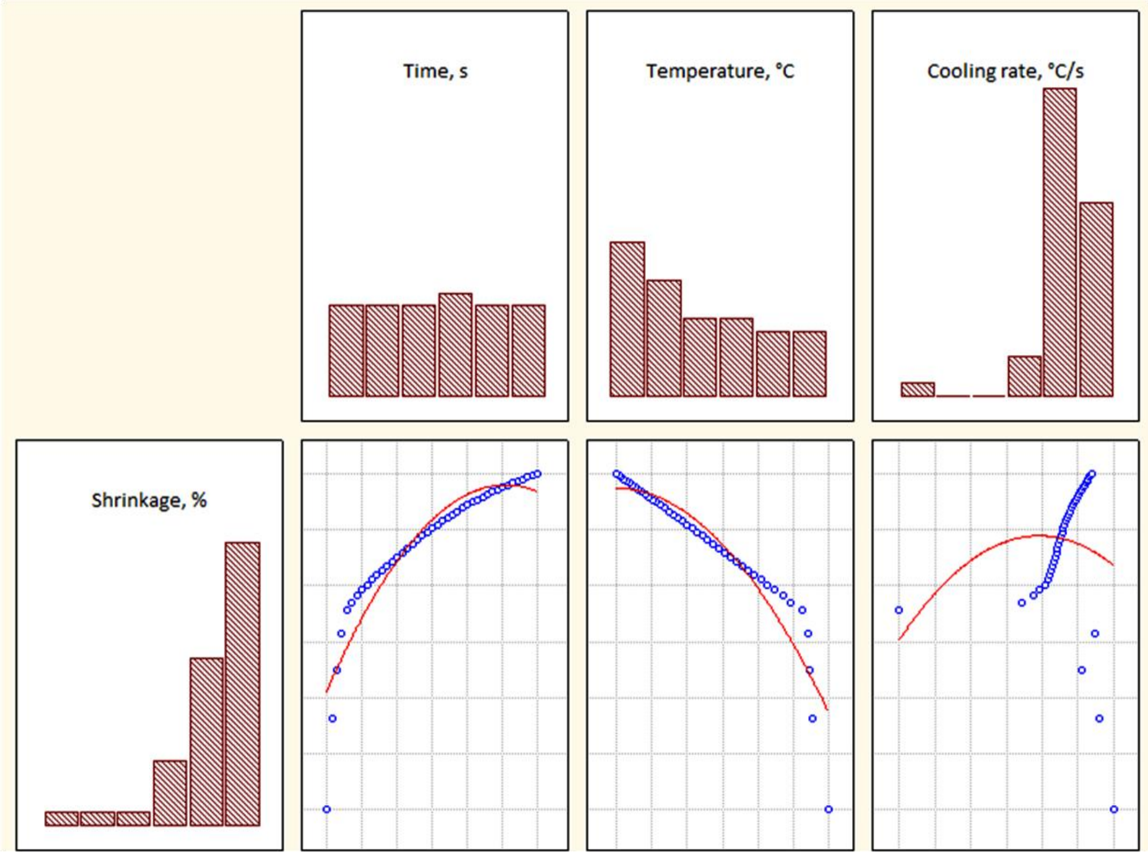

Regression equations (Matrix plot)

$$\begin{cases} \varepsilon = 4.01552755 + 0.0011598927t \\ \varepsilon = 9.60506748 - 0.00397917682T \\ \varepsilon = 6.7749948 + 1.1108003v \end{cases} \quad (6)$$

Figure 4 – The dependencies of shrinkage of corrosion-resistant steel X3CrNiMo18-12 from temperature, time and cooling rate. *t* – time, s; *v* – cooling rate, °C/s; *T* – temperature, °C.

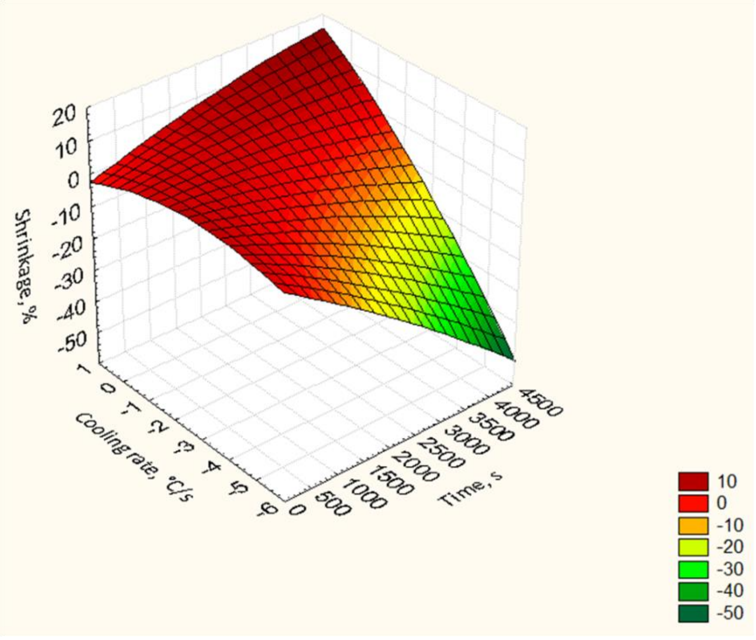

Regression equation (3D surface plot)

$$\varepsilon = 1.3302 + 0.0037t - 3.3956v - 4.4332 \cdot 10^{-7}t^2 + 0.0024tv - 0.5043v^2 \qquad (7)$$

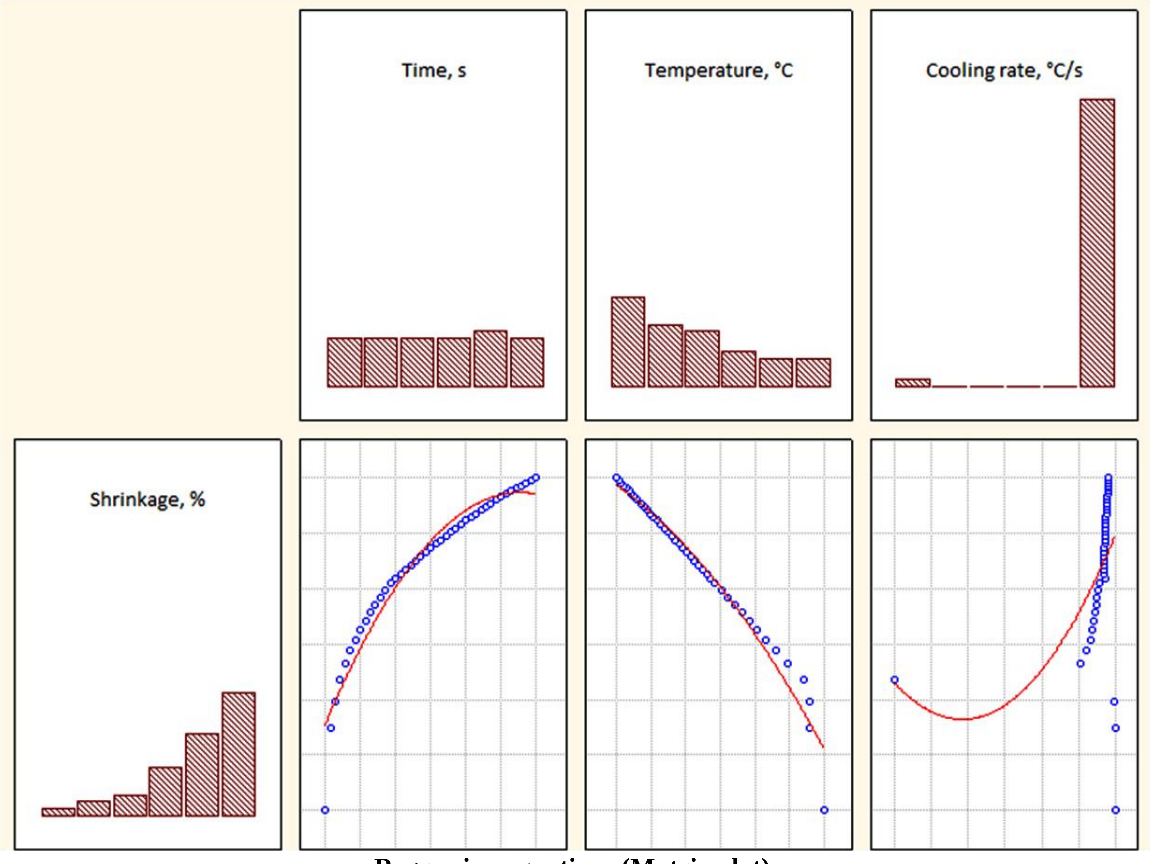

Regression equations (Matrix plot)

$$\begin{cases} \varepsilon = 3.33105561 + 0.00140749341t \\ \varepsilon = 10.1931941 - 0.00506379428T \\ \varepsilon = 6.56487773 + 0.743463575v \end{cases} \qquad (8)$$

Figure 5 – The dependencies of shrinkage of chromium steel SIS.2302 from temperature, time and cooling rate. *t* – time, s; *v* – cooling rate, °C/s; *T* – temperature, °C.

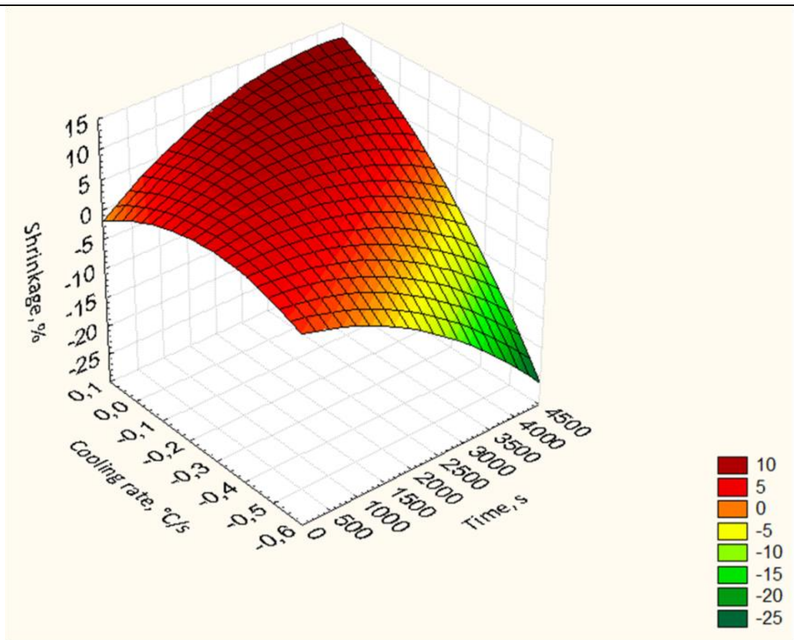

Regression equation (3D surface plot)

$$\varepsilon = 1.2328 + 0.006t - 27.1118v - 9.2426 \cdot 10^{-7}t^2 + 0.0135tv - 43.305v^2 \qquad (9)$$

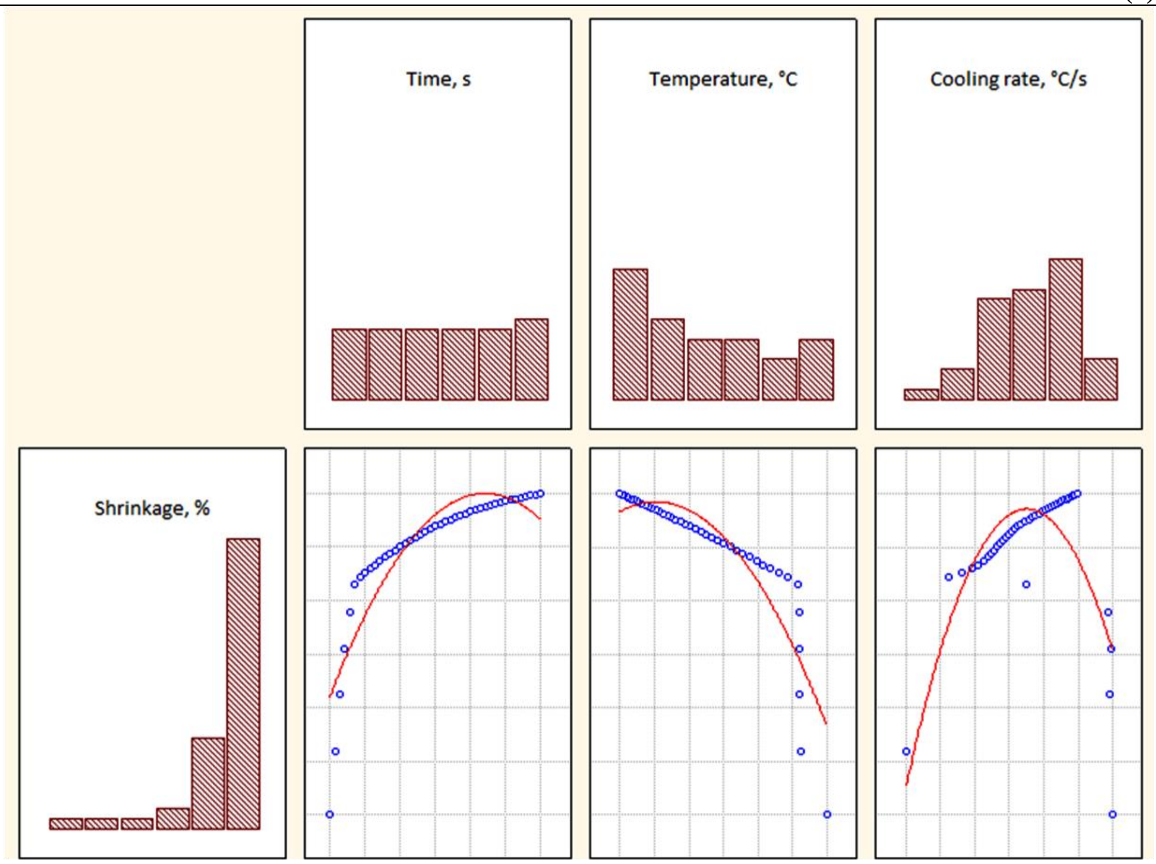

Regression equations (Matrix plot)

$$\begin{cases} \varepsilon = 4.08983099 + 0.000970201686t \\ \varepsilon = 8.61963292 - 0.00403275294T \\ \varepsilon = 6.27619729 + 0.667016445v \end{cases} \qquad (10)$$

Figure 6 – The dependencies of shrinkage of grey cast iron EN-GJL-150 from temperature, time and cooling rate. *t* – time, s; *v* – cooling rate, °C/s; *T* – temperature, °C.

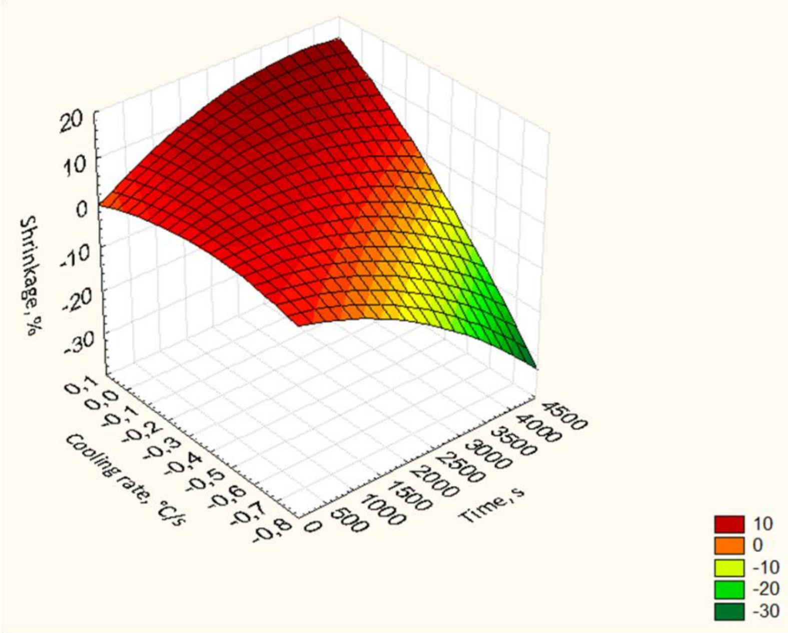

Regression equation (3D surface plot)

$$\varepsilon = 1.5695 + 0.0072t - 18.549v - 1.1149 \cdot 10^{-6}t^2 + 0.0127tv - 21.3591v^2 \quad (11)$$

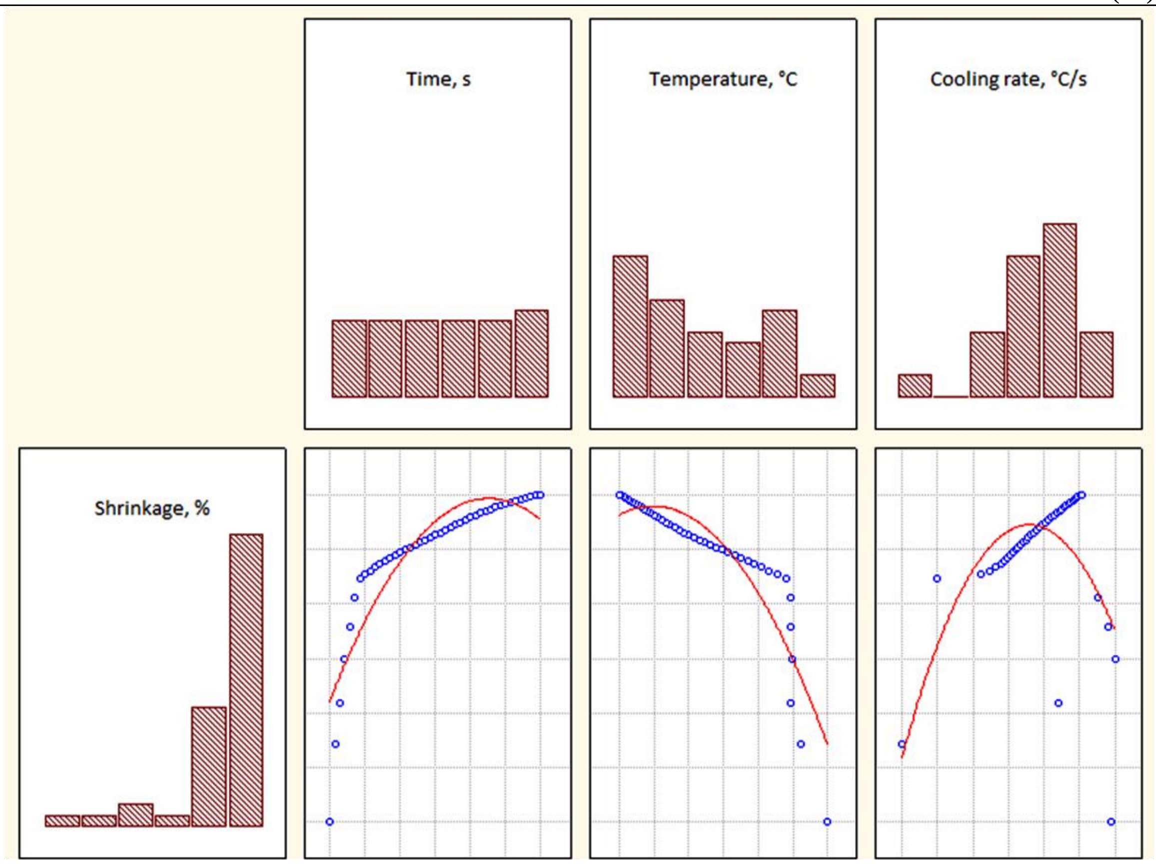

Regression equations (Matrix plot)

$$\begin{cases} \varepsilon = 4.98223975 + 0.0011991263t \\ \varepsilon = 10.5728911 - 0.00488327452T \\ \varepsilon = 7.88549675 + 1.64814752v \end{cases} \quad (12)$$

Figure 7 – The dependencies of shrinkage of malleable cast iron EN-JGS-600-3 from temperature, time and cooling rate. *t* – time, s; *v* – cooling rate, °C/s; *T* – temperature, °C.

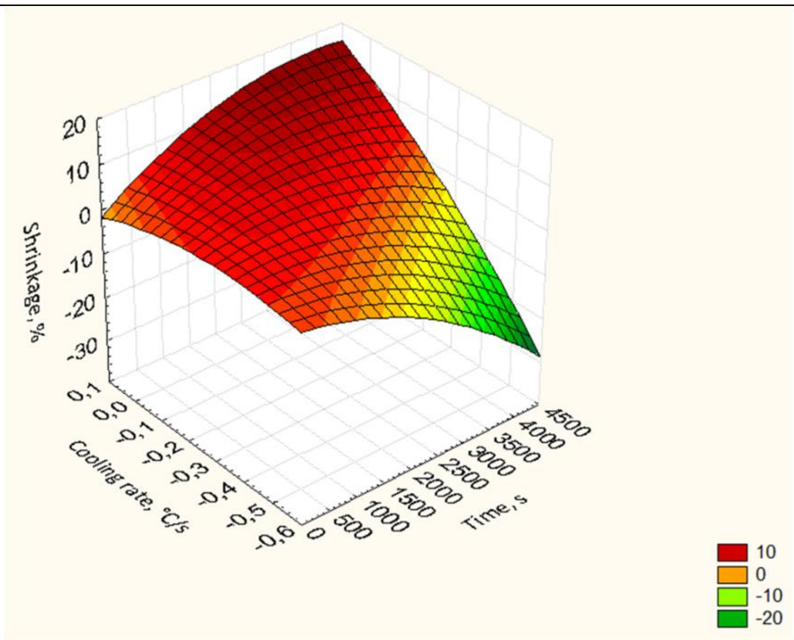

Regression equation (3D surface plot)

$$\varepsilon = 0.8066 + 0.0076t - 20.6186v - 1.1619 \cdot 10^{-6}t^2 + 0.0156tv - 28.6702v^2 \qquad (13)$$

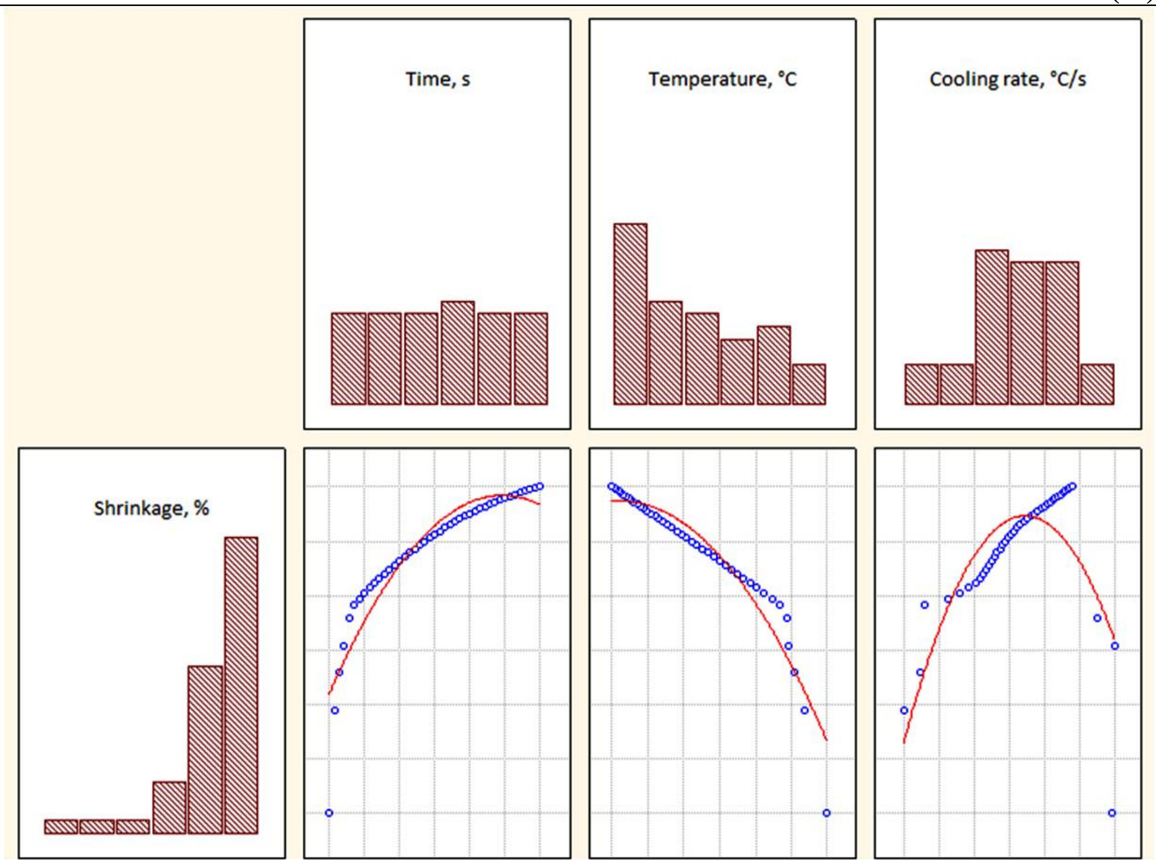

Regression equations (Matrix plot)

$$\begin{cases} \varepsilon = 3.65724356 + 0.000988982211t \\ \varepsilon = 8.31882395 - 0.00378237165T \\ \varepsilon = 6.53997955 + 3.17017395v \end{cases} \qquad (14)$$

Figure 8 – The dependencies of shrinkage of ductile cast iron EN-GJMW-210 from temperature, time and cooling rate. *t* – time, s; *v* – cooling rate, °C/s; *T* – temperature, °C.

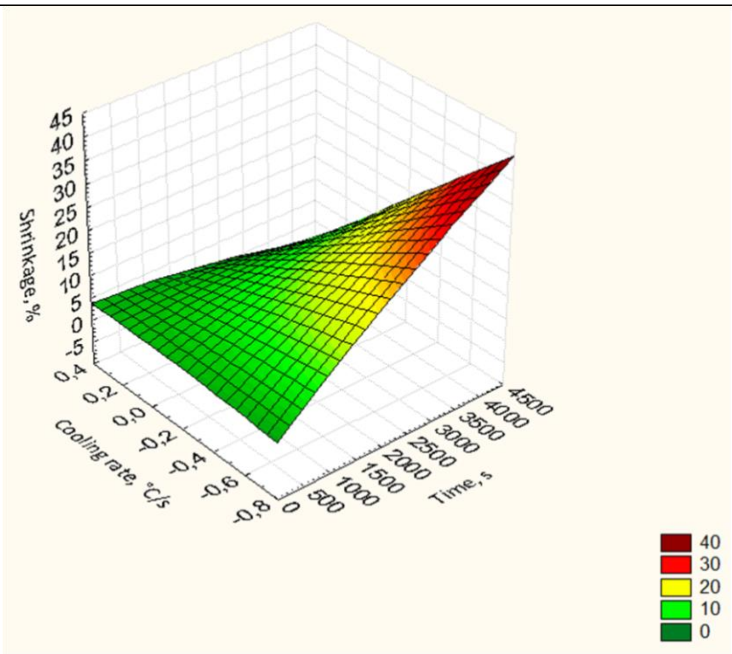

Regression equation (3D surface plot)

$$\varepsilon = 3.8766 + 0.0029t + 0.4141v - 3.0643 \cdot 10^{-7}t^2 - 0.0085tv - 1.606v^2 \quad (15)$$

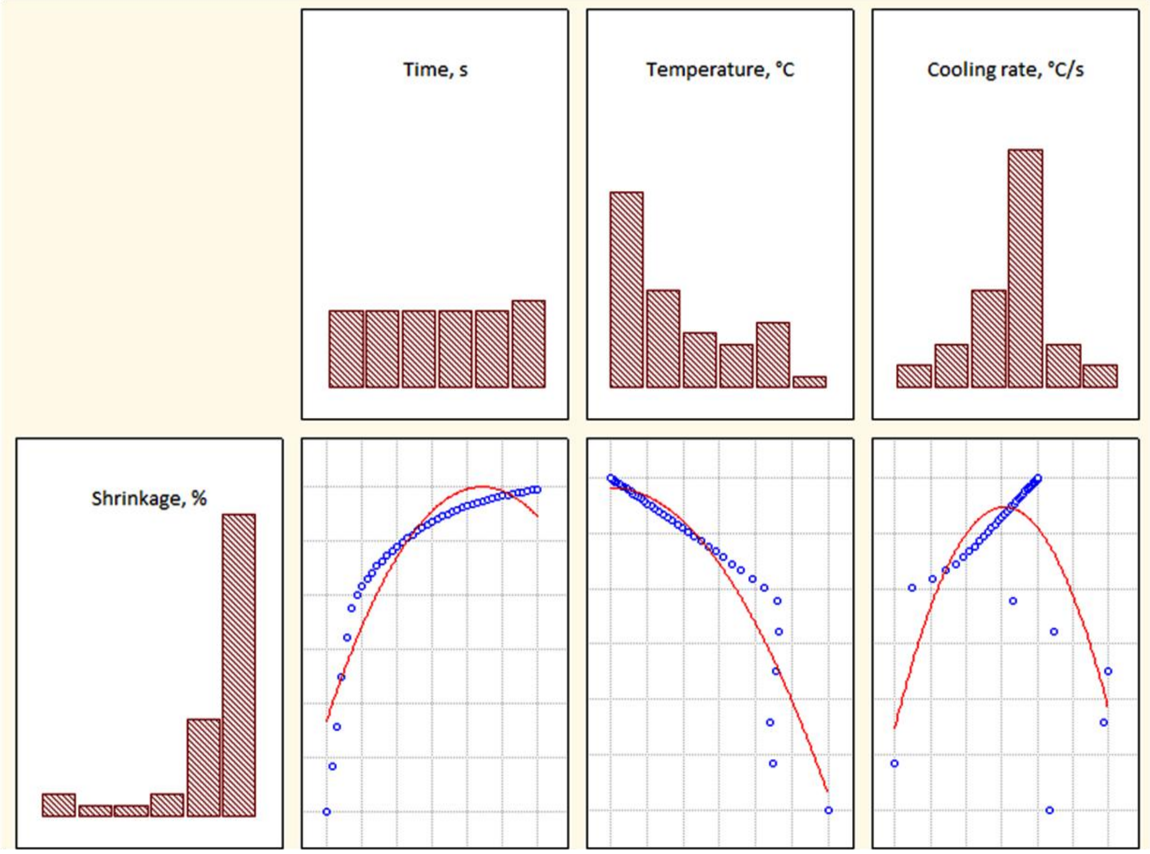

Regression equations (Matrix plot)

$$\begin{cases} \varepsilon = 6.46990704 + 0.00195161518t \\ \varepsilon = 14.5458981 - 0.00949729697T \\ \varepsilon = 10.8052545 + 1.28090503v \end{cases} \quad (16)$$

Figure 9 – The dependencies of shrinkage of tinless bronze CuAl10Fe2-C from temperature, time and cooling rate. *t* – time, s; *v* – cooling rate, °C/s; *T* – temperature, °C.

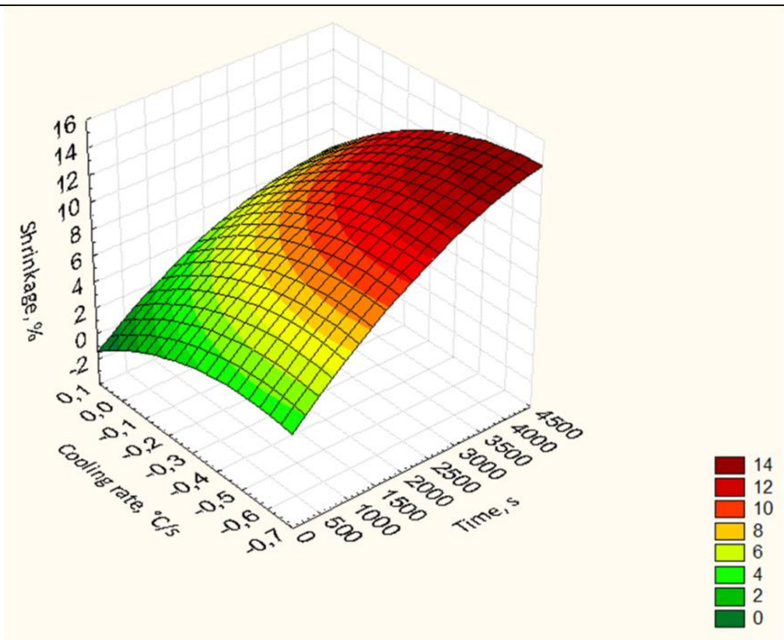

Regression equation (3D surface plot)

$$\varepsilon = -0.0164 + 0.0034t - 12.5216v - 3.5272 \cdot 10^{-7}t^2 - 0.0009tv - 11.6014v^2 \quad (17)$$

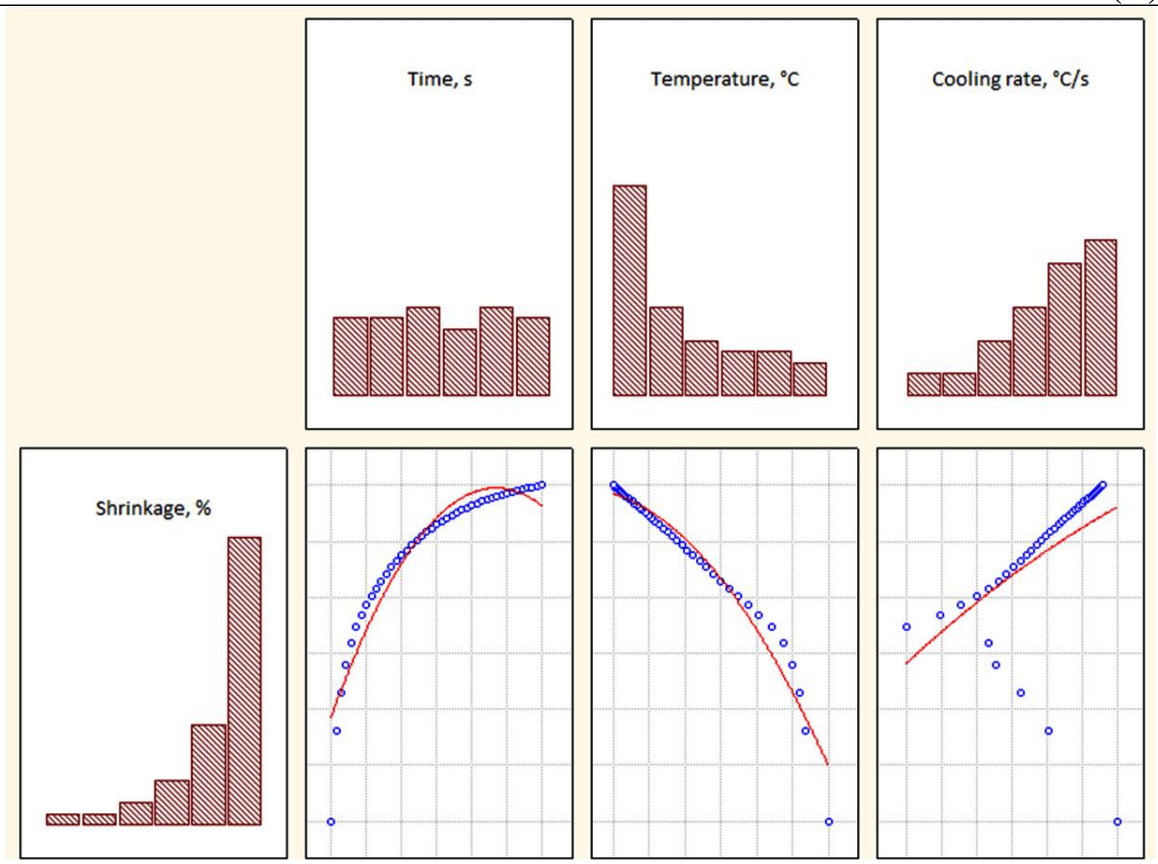

Regression equations (Matrix plot)

$$\begin{cases} \varepsilon = 4.41044314 + 0.00135374057t \\ \varepsilon = 9.87640709 - 0.00644338466T \\ \varepsilon = 8.56331029 + 6.15739118v \end{cases} \quad (18)$$

Figure 10 – The dependencies of shrinkage of tin bronze CuSn5Zn5Pb5-C from temperature, time and cooling rate. *t* – time, s; *v* – cooling rate, °C/s; *T* – temperature, °C.

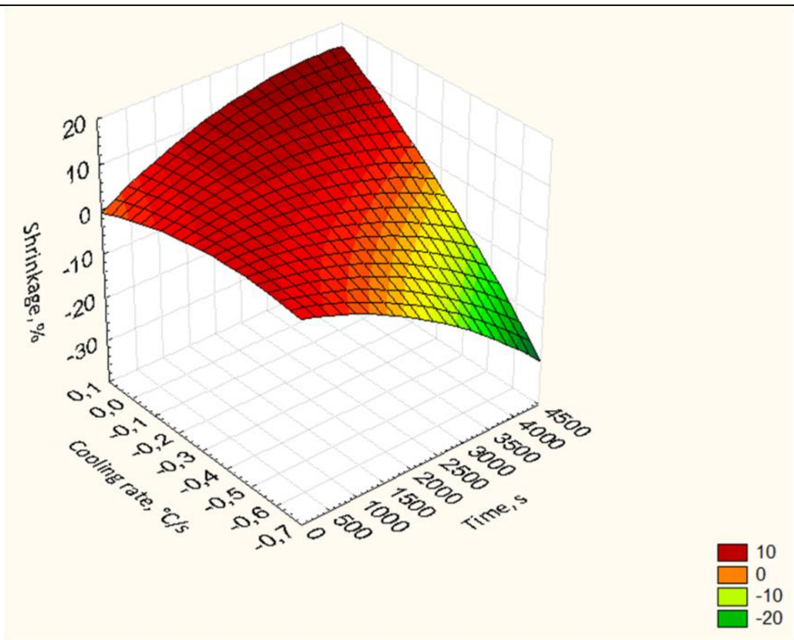

Regression equation (3D surface plot)

$$\varepsilon = 1.6529 + 0.0062t - 20.57v - 9.253 \cdot 10^{-7}t^2 + 0.0141tv - 21.0328v^2 \quad (19)$$

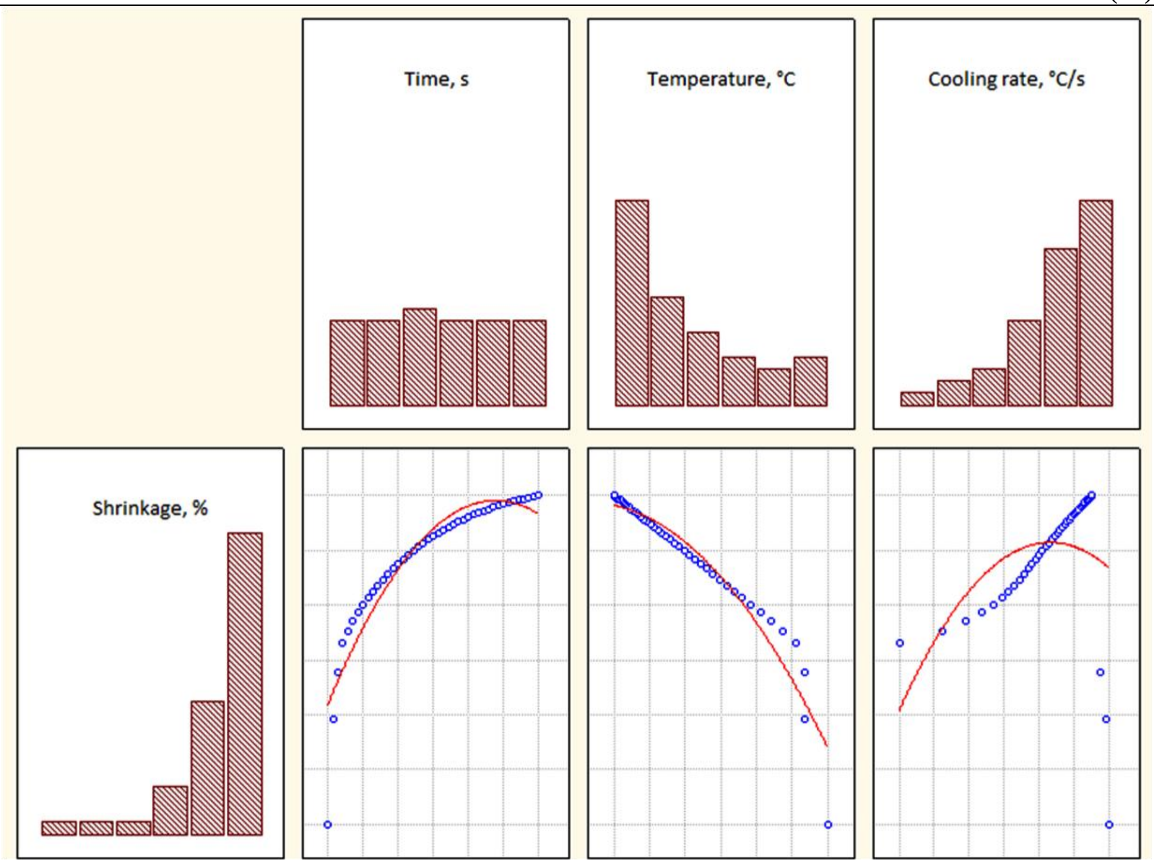

Regression equations (Matrix plot)

$$\begin{cases} \varepsilon = 5.02745177 + 0.00132987274t \\ \varepsilon = 10.6674125 - 0.00720113657T \\ \varepsilon = 8.56528215 + 4.0225989v \end{cases} \quad (20)$$

Figure 11 – The dependencies of shrinkage of brass CuZn40 from temperature, time and cooling rate. *t* – time, s; *v* – cooling rate, °C/s; *T* – temperature, °C.

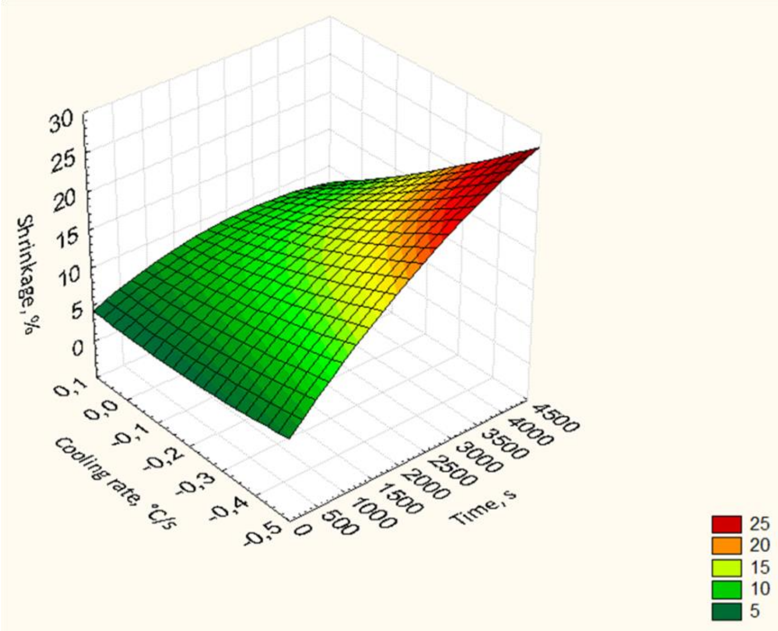

Regression equation (3D surface plot)

$$\varepsilon = 4.0402 + 0.0038t + 0.8393v - 5.1061 \cdot 10^{-7}t^2 - 0.0071tv + 9.0459v^2 \quad (21)$$

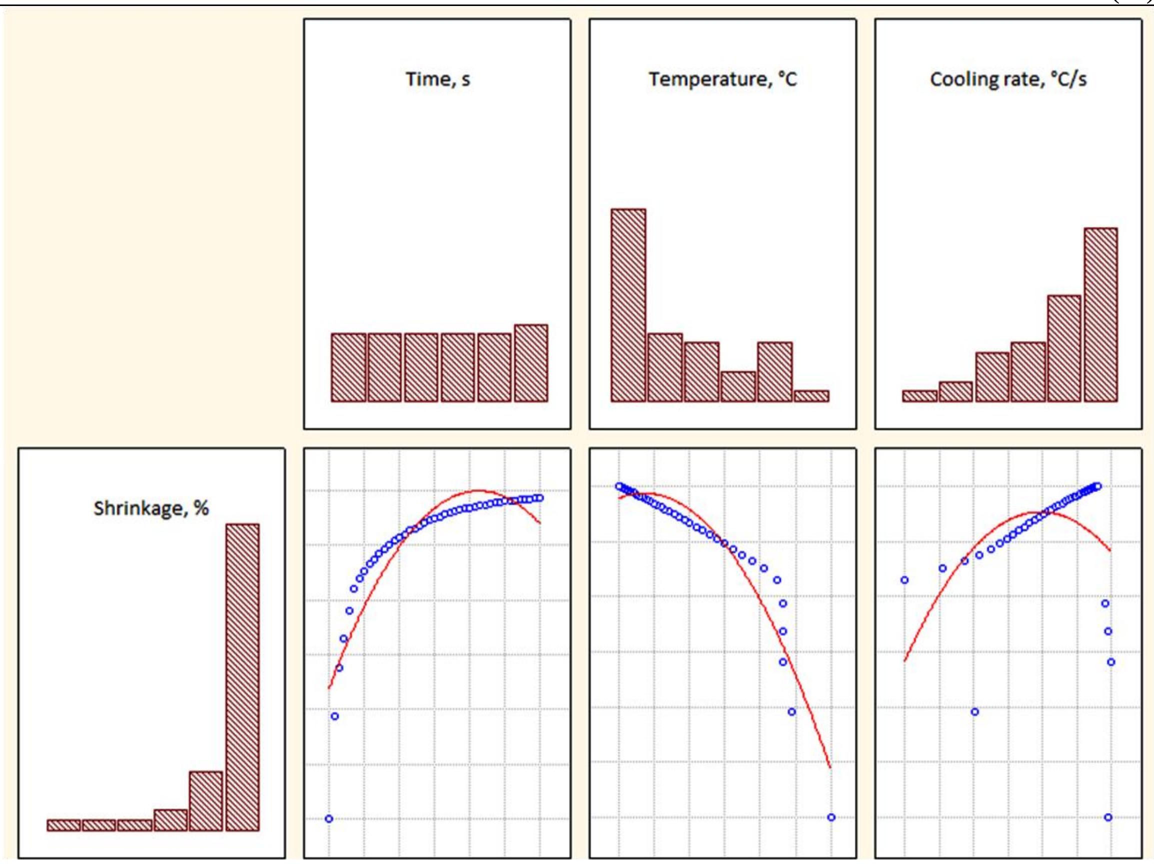

Regression equations (Matrix plot)

$$\begin{cases} \varepsilon = 7.32902904 + 0.00148110297t \\ \varepsilon = 13.3103426 - 0.0114417299T \\ \varepsilon = 10.9071908 + 3.60860387v \end{cases} \quad (22)$$

Figure 12 – The dependencies of shrinkage of aluminium foundry alloy SG 70A from temperature, time and cooling rate. *t* – time, s; *v* – cooling rate, °C/s; *T* – temperature, °C.

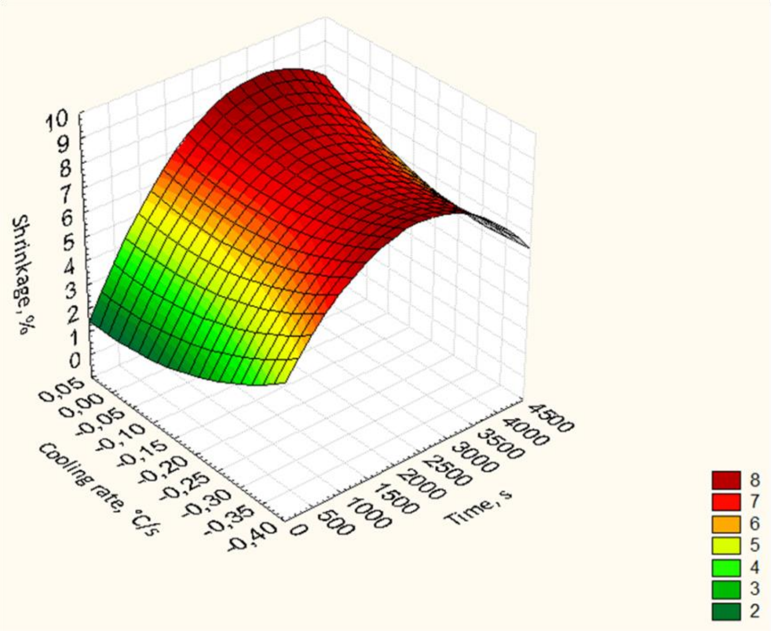

Regression equation (3D surface plot)

$$\varepsilon = 1.4574 + 0.0043t - 0.8618v - 6.9425 \cdot 10^{-7}t^2 + 0.0026tv + 17.905v^2 \quad (23)$$

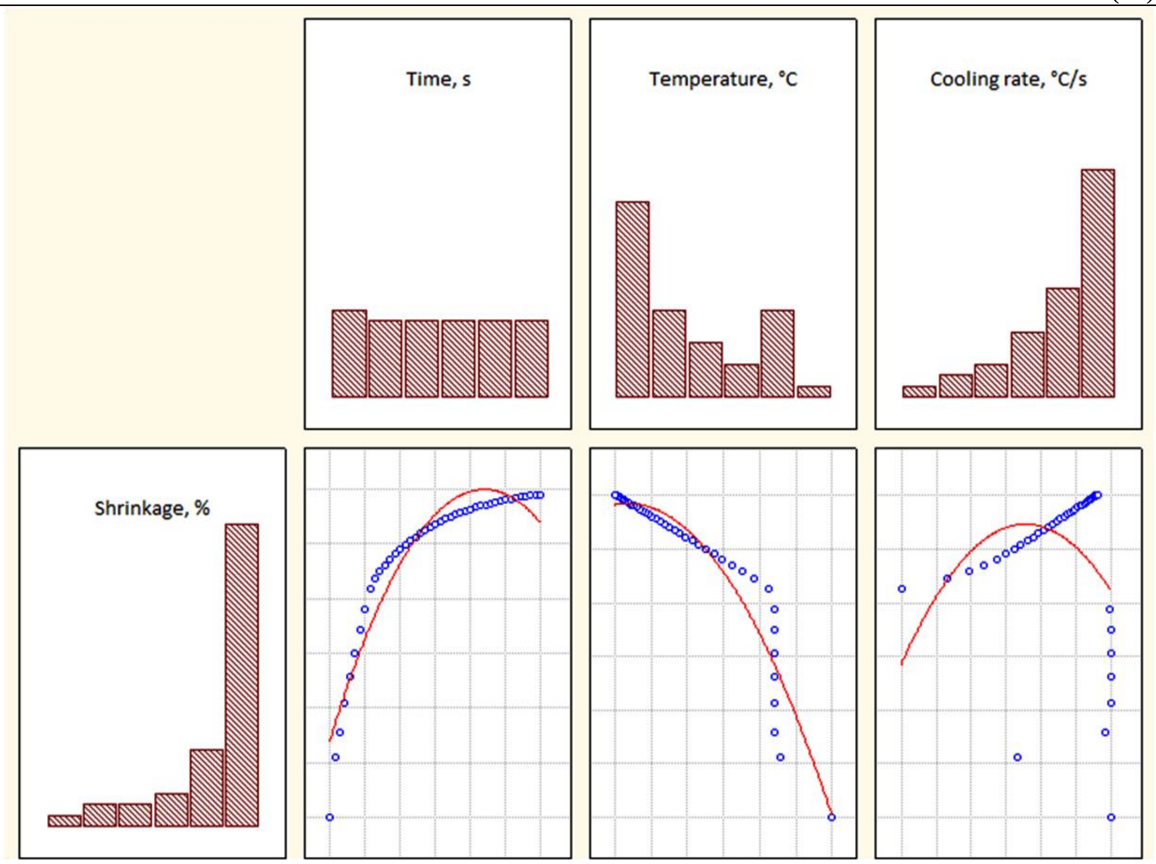

Regression equations (Matrix plot)

$$\begin{cases} \varepsilon = 3.72702338 + 0.00126424406t \\ \varepsilon = 8.99667115 - 0.0133797813T \\ \varepsilon = 6.30792829 - 0.908663887v \end{cases} \quad (24)$$

Figure 13 – The dependencies of shrinkage of zinc alloy ZA-8 from temperature, time and cooling rate. *t* – time, s; *v* – cooling rate, °C/s; *T* – temperature, °C.

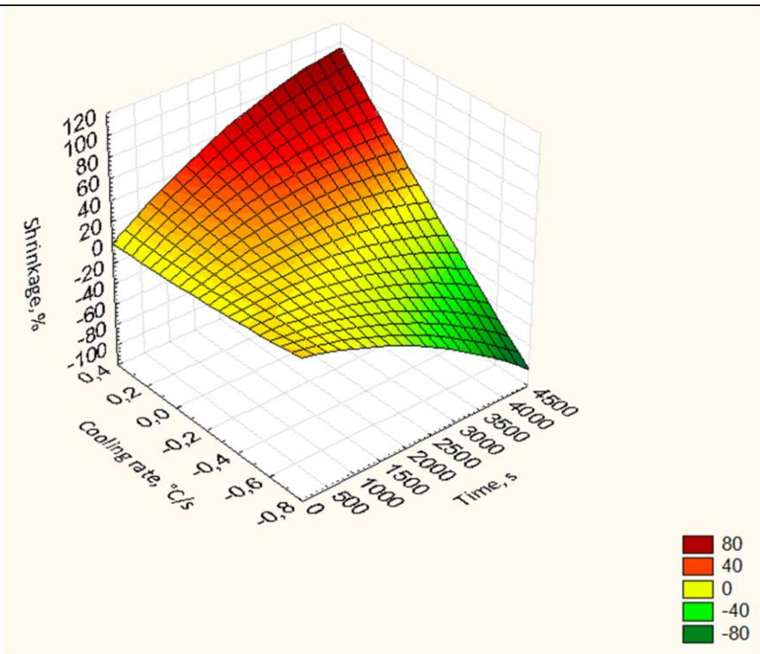

Regression equation (3D surface plot)

$$\varepsilon = 1.4694 + 0.0204t - 9.6807v - 3.3051 \cdot 10^{-6}t^2 + 0.0398tv + 8.7557v^2 \quad (25)$$

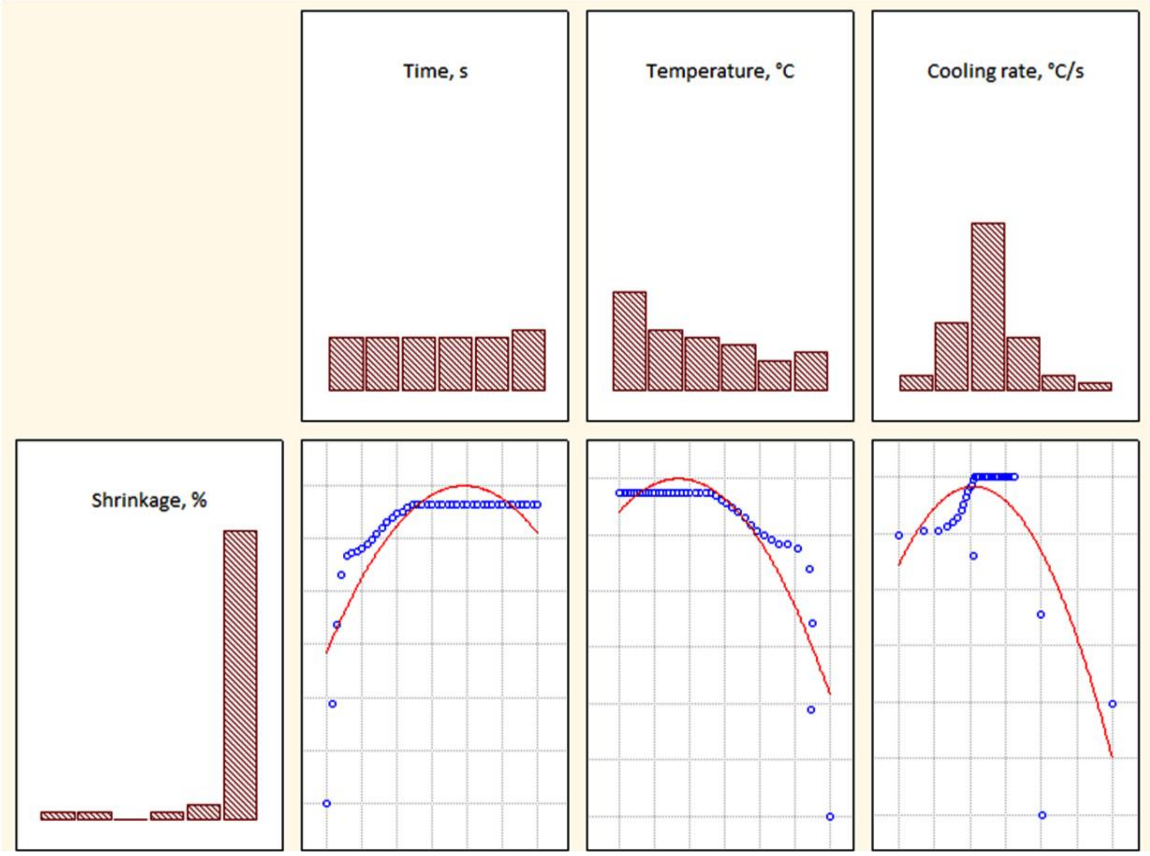

Regression equations (Matrix plot)

$$\begin{cases} \varepsilon = 6.80536394 + 0.000893767752t \\ \varepsilon = 11.3542006 - 0.00339502082T \\ \varepsilon = 7.56808072 - 4.27127712v \end{cases} \quad (26)$$

Figure 14 – The dependencies of shrinkage of nickel-cobalt alloy num.1 from temperature, time and cooling rate. *t* – time, s; *v* – cooling rate, °C/s; *T* – temperature, °C.

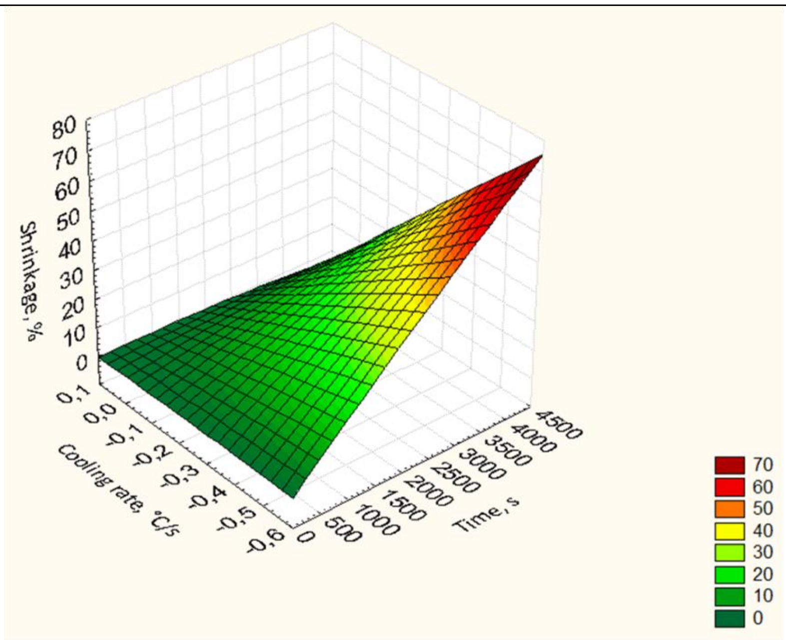

Regression equation (3D surface plot)

$$\varepsilon = -0.0336 + 0.0031t - 2.8646v - 2.6444 \cdot 10^{-7}t^2 - 0.0246tv - 3.7317v^2 \quad (27)$$

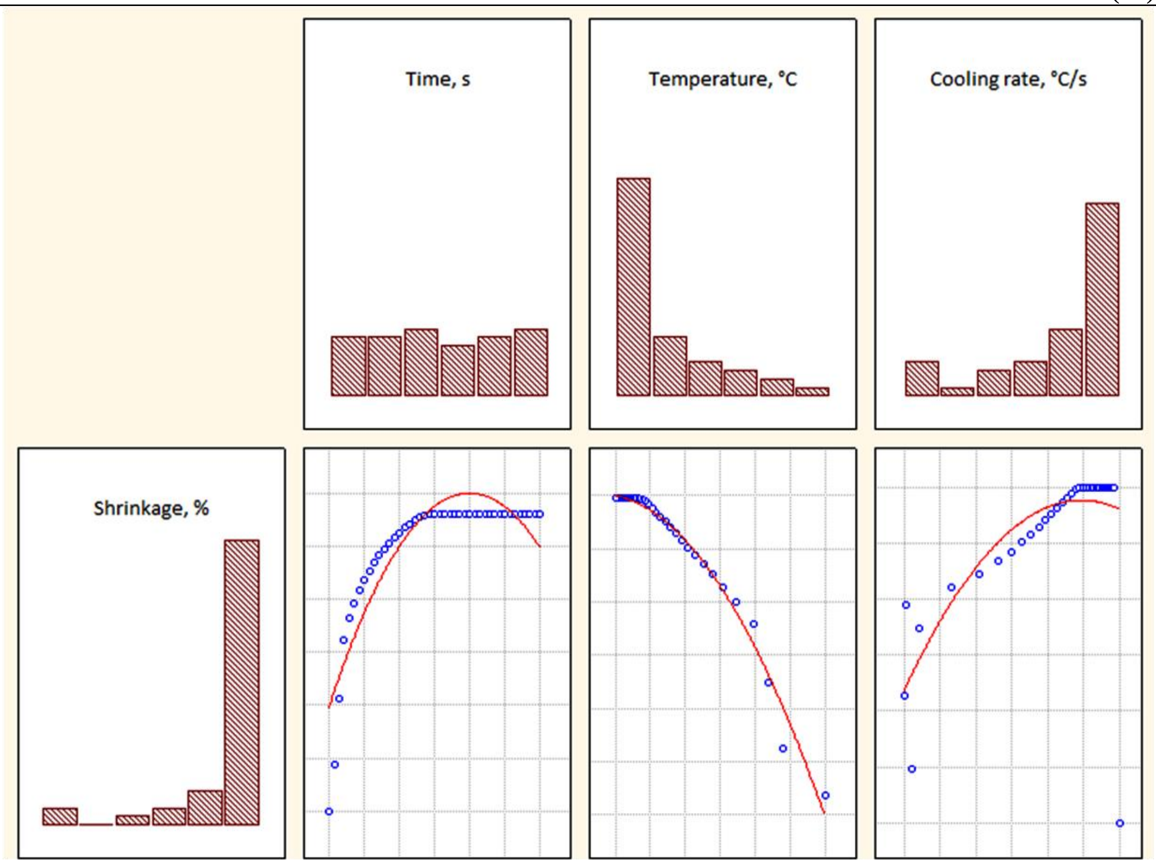

Regression equations (Matrix plot)

$$\begin{cases} \varepsilon = 5.79711189 + 0.00120125523t \\ \varepsilon = 10.4250495 - 0.012273746T \\ \varepsilon = 9.53667192 + 9.45672317v \end{cases} \quad (28)$$

Figure 15 – The dependencies of shrinkage of magnesium alloy MAG2 from temperature, time and cooling rate. *t* – time, s; *v* – cooling rate, °C/s; *T* – temperature, °C.

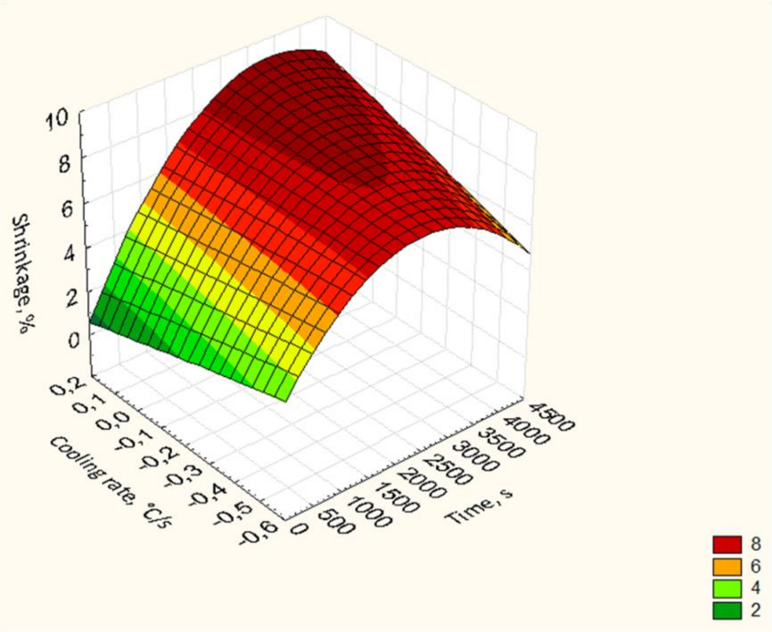

Regression equation (3D surface plot)

$$\varepsilon = 1.2987 + 0.0046t - 3.5925v - 7.2614 \cdot 10^{-7}t^2 + 0.0018tv - 0.3205v^2 \quad (29)$$

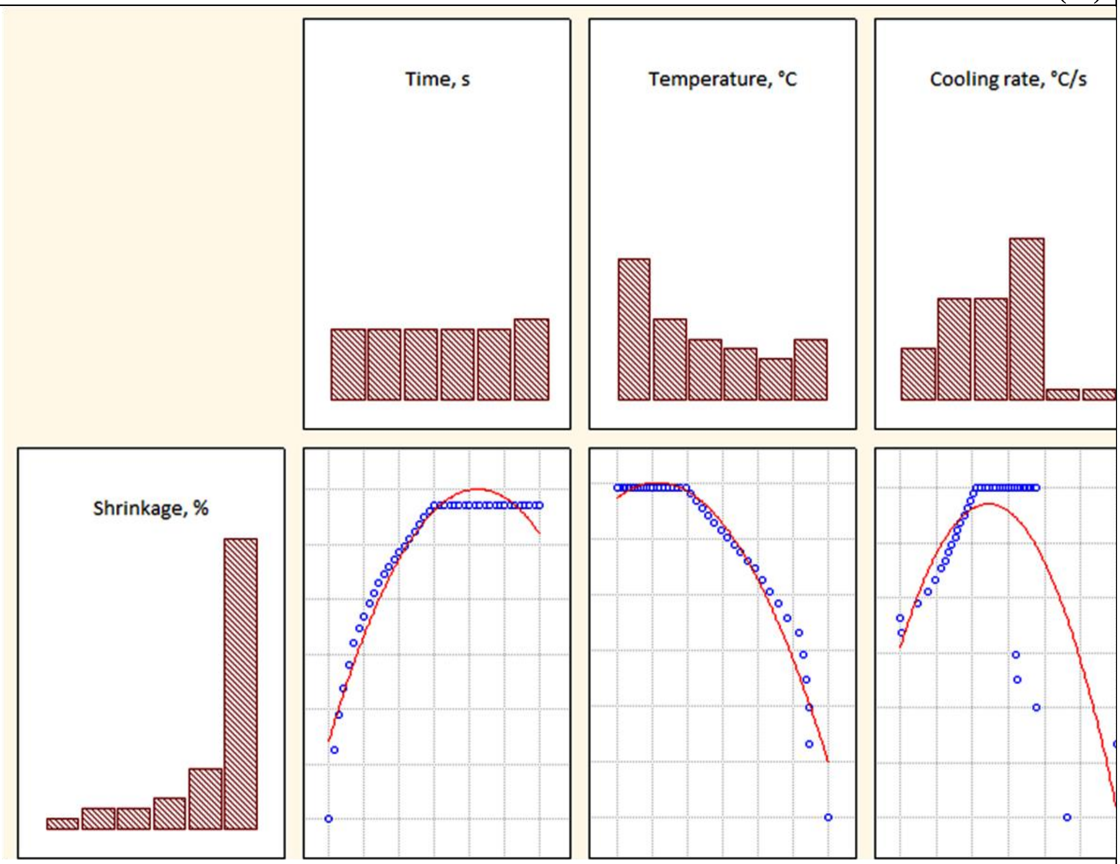

Regression equations (Matrix plot)

$$\begin{cases} \varepsilon = 4.11244534 + 0.00126616878t \\ \varepsilon = 9.92689673 - 0.00456210614T \\ \varepsilon = 6.45539702 - 1.22171003v \end{cases} \quad (30)$$

Figure 16 – The dependencies of shrinkage of nickel alloy NiCr20TiAl from temperature, time and cooling rate. *t* – time, s; *v* – cooling rate, °C/s; *T* – temperature, °C.

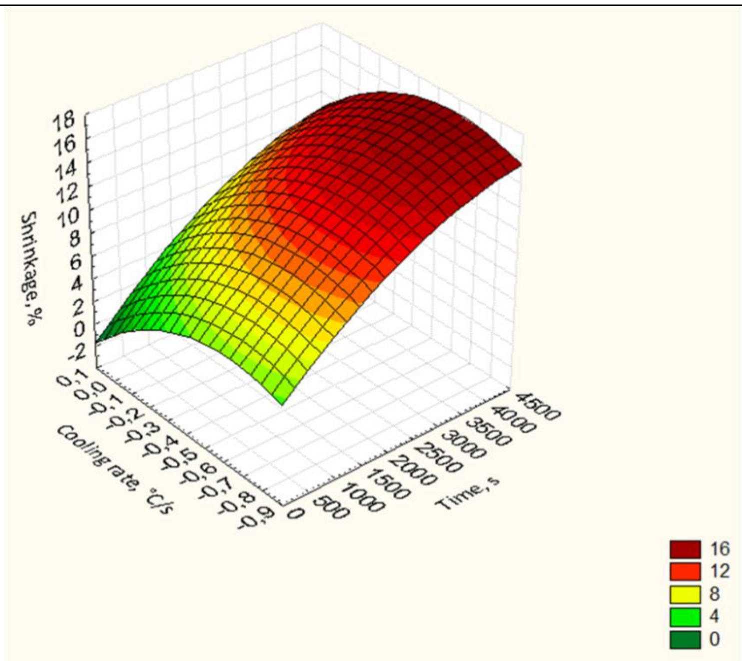

Regression equation (3D surface plot)

$$\varepsilon = 0.0847 + 0.0045t - 16.7225v - 4.1136 \cdot 10^{-7}t^2 + 0.0003tv - 12.9696v^2 \quad (31)$$

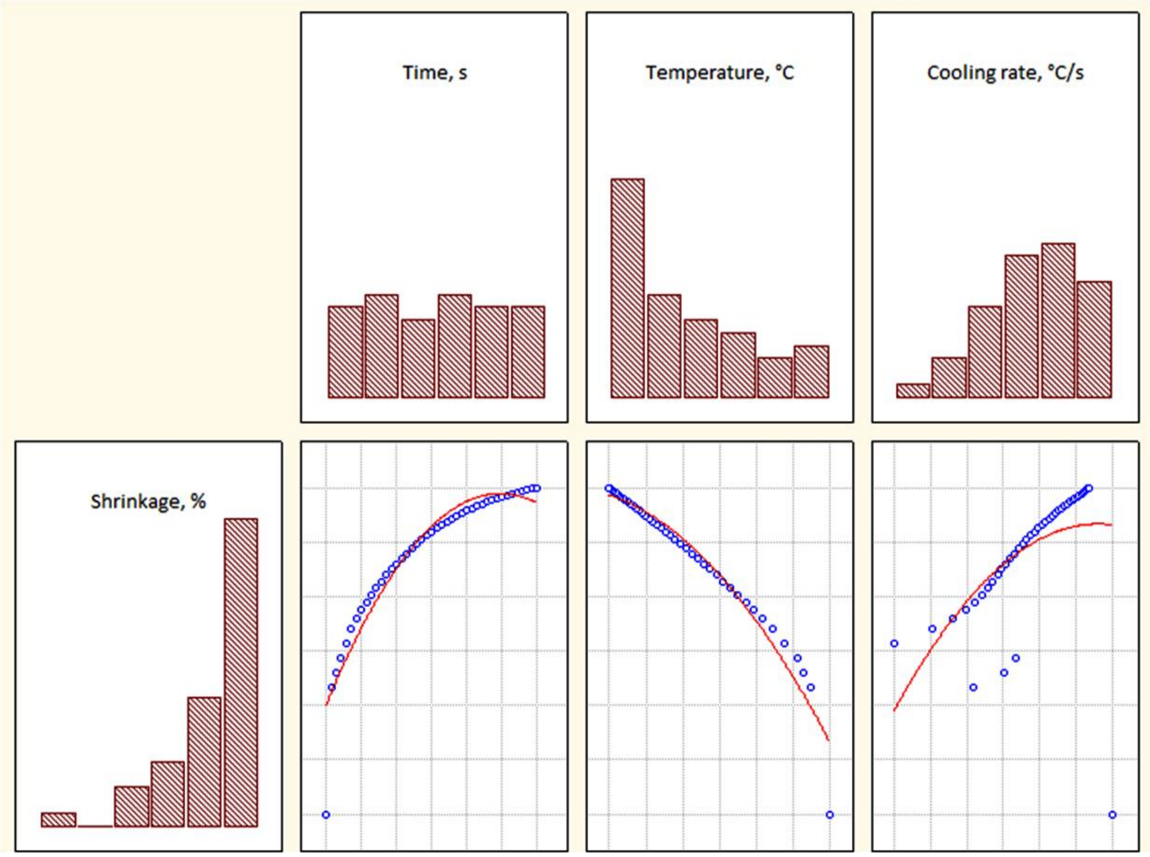

Regression equations (Matrix plot)

$$\begin{cases} \varepsilon = 6.42167609 + 0.001936747 31t \\ \varepsilon = 14.4680144 - 0.00643984218T \\ \varepsilon = 12.8833113 + 7.96157659v \end{cases} \quad (32)$$

Figure 17 – The dependencies of shrinkage of soft magnetic alloy 49K2FA from temperature, time and cooling rate. *t* – time, s; *v* – cooling rate, °C/s; *T* – temperature, °C.

Volumetric shrinkage of alloys (in the liquid state) has the following calculated values: alloy steel 34CrMo4 – 2.87 %, carbon steel 1.0503 – 2.34 %, corrosion-resistant steel X3CrNiMo18-12 – 2.22 %, chromium steel SIS.2302 – 2.09 %, grey cast iron EN-GJL-150 – 1.43 %, malleable cast iron EN-JGS-600-3 – 2.18 %, ductile cast iron EN-GJMW-210 – 2.24 %, tinless bronze CuAl10Fe2-C – 1.8 %, tin bronze CuSn5Zn5Pb5-C – 2.42 %, brass CuZn40 – 3.06 %, aluminium foundry alloy SG 70A – 3.86 %, zinc alloy ZA-8 – 1.46 %, nickel-cobalt alloy num.1 – 3.12 %, magnesium alloy MAG2 – 1.48 %, nickel alloy NiCr20TiAl – 1.78 %, soft magnetic alloy 49K2FA – 5.13 %.

Conclusion

According to the polynomial and linear regression equations and the two-dimensional (three-dimensional) plots it can be inferred by character of the cooling process of the castings made of different metallic alloys. The mathematical signs in the regression equations («plus» or «minus») are indicated to the increase or decrease of alloy temperature, time and cooling rate. The forecast of the change of the melts volumes was performed according to the calculated values of volumetric shrinkage. The minimum decrease of the volume was defined for gray cast iron, zinc and magnesium alloys.

References:

1. Larichev NS, Korotchenko AYu, Kutsaya AYu (2016) Assessment of the impact of constrained shrinkage on the formation of porosity in castings. Foundry. Technologies and Equipment, vol. 7. – pp. 10 – 15.
2. Trukhov AP (2008) Linear shrinkage and precision of sizes of castings manufactured in green sand molds. Scientific Technical and Production Journal «Blanking Productions in Mechanical Engineering», vol. 1. – pp. 4 – 7.
3. Matveev IA (2011) Prediction of shrinkage deformation of steel castings during cooling. Russian Foundry man, vol. 2. – pp. 22 – 25.
4. Hangai Y, Yano T, Murata Y, Kuwazuru O, Utsunomiya T, Kitahara S, Bidhar S, Yoshikawa N (2010) Clustered shrinkage pores in ill-conditioned aluminum alloy die castings. Materials Transactions, vol. 51, № 9. – pp. 1574 – 1580.
5. Chemezov D (2017) Shrinkage of some metal alloys after solidification. ISJ Theoretical & Applied Science, 06 (50): 87-89. Soi: http://s-o-i.org/1.1/TAS-06-50-10 Doi: https://dx.doi.org/10.15863/TAS.2017.06.50.10
6. Chemezov D (2017) The degree of shrinkage porosity in the castings after solidification. ISJ Theoretical & Applied Science, 07 (51): 1-6. Soi: http://s-o-i.org/1.1/TAS-07-51-1 Doi: https://dx.doi.org/10.15863/TAS.2017.07.51.1
7. Chemezov D, Bayakina A, Bogomolova E, Lukyanova T (2017) To the question of the solidification process of steel castings with different wall thicknesses. ISJ Theoretical & Applied Science, 03 (47): 38-41. Soi: http://s-o-i.org/1.1/TAS-03-47-8 Doi: https://dx.doi.org/10.15863/TAS.2017.03.47.8
8. Kuang-Oscar Yu (2001) Modeling for Casting and Solidification Processing. CRC Press. – 703 p.
9. Roux P, Goyeau B, Gobin D, Fichot F, Quintard M (2006) Chemical non-equilibrium modeling of columnar solidification. International Journal of Heat and Mass Transfer 49(23-24). – pp. 4496 – 4510.